Multi-Stream Transmission in Cell-Free MIMO Networks with Coherent AP Clustering

Esra Aycan Beyazıt, Jeroen Famaey, Nina Slamnik-Kriještorac, Johann M. Marquez-Barja, Miguel Camelo Botero
University of Antwerp - imec, IDLab, Antwerp, Belgium
Email: {esra.aycanbeyazit, jeroen.famaey, nina.slamnik-krijestorac, johann.marquez-barja, miguel.camelobotero}@uantwerpen.be

***Abstract*—This letter proposes a multi-stream selection framework for Cell-Free Multiple-Input Multiple-Output (CF-MIMO) networks. Partially coherent transmission has been considered by clustering Access Points (APs) into phase-aligned clusters to address the challenges of phase misalignment and inter-cluster interference. A novel stream selection algorithm is developed to dynamically allocate multiple streams to each multi-antenna User Equipment (UE), ensuring that the system optimizes the sum rate while minimizing inter-cluster and inter-stream interference. Numerical results validate the effectiveness of the proposed method in enhancing spectral efficiency and fairness in distributed CF-MIMO networks.**

***Keywords*—CF-MIMO, stream selection, coherent and non-coherent transmissions, and interference mitigation.**

I. Introduction

The deployment of CF-MIMO has emerged as a key enabler for next-generation wireless networks, offering substantial improvements in spectral efficiency, energy efficiency, and uniform user coverage by eliminating cell boundaries [1]. In CF-MIMO networks, a large number of geographically distributed APs collaboratively serve UEs on the same time-frequency resources, achieving high data rates through coherent transmission [2], [3]. However, practical limitations such as hardware imperfections, synchronization errors, and varying propagation delays introduce phase misalignment among APs, significantly impacting the effectiveness of coherent operation. Specifically, these factors hinder accurate Channel State Information (CSI) acquisition and disrupt phase alignment, leading to severe degradation in the achievable rate of the network.

To address the challenges of phase misalignment and asynchronous reception, recent studies have proposed a mixed coherent and non-coherent transmission approach [4]. Since clustering APs within a small area enables coherent transmission [2], APs are grouped into phase-aligned clusters, where those within the same cluster perform coherent transmission, while transmission across clusters remains non-coherent. Such a hybrid strategy mitigates performance degradation caused by asynchronous reception by balancing the benefits of coherent transmission within clusters with the flexibility of non-coherent transmission between them.

Most state-of-the-art solutions [5]–[7] assume UEs are equipped with a single antenna in CF-MIMO networks, which limits their applicability in next-generation networks, where multi-antenna UEs are becoming increasingly common. When UEs are equipped with multiple antennas and multiple data streams are transmitted simultaneously, interference between these streams can significantly degrade overall system performance, especially in networks with non-coherent transmission regimes [4]. Consequently, managing inter-stream interference in non-coherent regimes is crucial to ensure that multi-stream transmissions provide a significant performance boost compared to single-stream transmissions [8]. Stream selection based on Interference Alignment (IA) was initially studied in conventional and heterogeneous cellular networks [9], [10]. However, despite its importance for enhancing spectral efficiency, determining the optimal number of streams for each UE and selecting the best stream combinations in CF-MIMO networks remains underexplored.

To address these challenges, this paper investigates multi-stream selection in CF-MIMO networks with mixed coherent and non-coherent transmission. We first analyze the impact of multi-stream transmission in partially coherent CF-MIMO systems, examining how clustering and transmission strategies affect spectral efficiency and inter-cluster interference. Therefore, we propose a dynamic stream allocation algorithm that optimally assigns data streams to UEs equipped with multiple antennas. The approach jointly computes precoding and decoding matrices to maximize spectral efficiency while ensuring each UE receives at least one stream. Stream sequences are initialized with the strongest streams from each cluster-UE pair and compared to determine the sequence achieving the highest sum rate. The framework dynamically adjusts the number of streams per UE based on network conditions, balancing throughput and interference mitigation. The proposed algorithm is evaluated through extensive numerical simulations under diverse clustering scenarios, comparing it to both an upper bound and a baseline. The upper bound is obtained via an exhaustive search of all possible stream combinations, identifying the optimal sequence. The baseline follows a greedy approach, constructing a single stream sequence by iteratively selecting the strongest streams for each UE to maximize spectral efficiency. Our method significantly improves spectral efficiency under severe phase misalignment and interference. Such conditions are especially challenging in densely deployed next-generation networks, where distributed architectures with partial synchronization offer a more flexible and scalable alternative to conventional methods.

Notations: $(\mathbf{A})^H$ denotes the conjugate transpose of a matrix $\mathbf{A}$. Capital Greek letters such as Ω denote sets, $|\Omega|$ indicates the number of elements in set Ω. The expectation operator is denoted by $\mathbb{E}\{\cdot\}$.

II. System Model

This study considers a CF-MIMO system with L APs, each with N_T transmit antennas, serving K UEs, each with N_R receive antennas. All APs are connected to a central processing unit (CPU) via fronthaul links. While full phase coherence is ideal, network-wide synchronization is impractical [2]. Thus, the network supports both coherent and non-coherent transmissions: APs within a cluster maintain phase alignment for coherent transmission, whereas inter-cluster transmissions remain non-coherent due to the lack of synchronization.

The system model for both transmission modes is defined as follows: Let $\mathcal{M}_k \subset \{1, \ldots, L\}$ denote the subset of APs serving UE k, referred to as clusters throughout this paper. A fully non-coherent transmission occurs when $|\mathcal{M}_k| = L$, meaning that no clustering is applied. Conversely, when $|\mathcal{M}_k| = 1$, a single large cluster enables fully coherent transmission.

A. Downlink Data Transmission

The considered phase-aligned transmission inside the clusters is achieved by forming a virtual large MIMO array, enabling the coherent transmission of data symbols [11]. Each cluster is associated with one UE. The set of UE-cluster pairs can be denoted as $k \in \Gamma = \{1, ..., K\}$. The implemented coherent AP clustering method is described in Section III-A.

If the c^{th} cluster is denoted by $\mathcal{M}_c$, in a coherent transmission, the channel between the subset of APs $\mathcal{M}_c$ and UE k is represented by the collective channel $\mathbf{H}_{k\mathcal{M}_c} \in \mathbb{C}^{N_R \times N_T|\mathcal{M}_c|}$, where $|\mathcal{M}_c|$ is the number of APs in cluster $\mathcal{M}_c$. The collective channel between cluster $\mathcal{M}_c$ and UE k can be expressed as:

$$\mathbf{H}_{k\mathcal{M}_c} = \begin{bmatrix} \mathbf{h}_{kl_1} & \mathbf{h}_{kl_2} & \cdots & \mathbf{h}_{kl_{|\mathcal{M}_c|}} \end{bmatrix}, \tag{1}$$

where $l_1, l_2, ..., l_{|\mathcal{M}_c|} \in \mathcal{M}_c$ and $\mathbf{h}_{kl} \in \mathbb{C}^{N_R \times N_T}$ represents the channel matrix from AP l to UE k, for all $l \in \mathcal{M}_c$. The output signal at user k is defined as follows.

$$\mathbf{y}_k = \alpha_{kk}\mathbf{H}_{k\mathcal{M}_k}\mathbf{x}_k + \sum_{\substack{j=1,\\ j\neq k}}^{K} \alpha_{kj}\mathbf{H}_{k\mathcal{M}_j}\mathbf{x}_j + \mathbf{n}_k \tag{2}$$

where, $\alpha_{kj}\mathbf{H}_{k\mathcal{M}_j}$ is the channel matrix between cluster $\mathcal{M}_j$ and UE k with dimension $N_R \times N_T|\mathcal{M}_j|$. Each element of $\mathbf{H}_{k\mathcal{M}_j}$ includes fading, modeled as an independent and identically distributed complex Gaussian random variable with $\mathcal{CN}(0, 1)$. α_{kj} is the large-scale fading coefficient and it can be modeled as $\alpha_{kl} = 10^{-\text{PL}(\text{dis}_{kl})/10}10^{-F_{kl}/10}$, where $\text{PL}(\text{dis}_{kl})$ represents the path loss function with the parameter of the distance between AP l and UE k, and F_{kl} is the shadowing effect [1]. For each receiver k, $\mathbf{n}_k$ is a $N_R \times 1$ vector. Each element of $\mathbf{n}_k$ represents additive white Gaussian noise with zero mean and variance of σ^2. $\mathbf{x}_{\mathcal{M}_k}$ is the transmitted signal from the $\mathcal{M}_k^{th}$ cluster with dimension $N_T|\mathcal{M}_k| \times 1$ and it is calculated as follows.

$$\mathbf{x}_{\mathcal{M}_k} = \sqrt{P_k}\mathbf{T}_{\mathcal{M}_k}\mathbf{s}_k \tag{3}$$

where P_k is the transmit power of AP k. $\mathbf{T}_{\mathcal{M}_k}$ is the unitary precoding matrix of cluster $\mathcal{M}_k$ with dimension $N_T|\mathcal{M}_k| \times q_k$, and cluster $\mathcal{M}_k$ can transmit q_k independent streams with $q_k \leq d_k$ where $d_k = \min(N_R, N_T|\mathcal{M}_k|)$. $\mathbf{s}_k$ is the symbol vector with dimension of $q_k \times 1$ and denoted as $\mathbf{s}_k = [s_{k,1} \ldots s_{k,q_k}]^T$ where $\mathbb{E}\left[\|\mathbf{s}_k\|^2\right] = 1$, and it is assumed that the transmit power is equally shared between the symbols, $\mathbb{E}\left[|s_{k,n}|^2\right] = 1/q_k$, $n = 1, ..., q_k$. The total number of streams in the network is calculated as $r = \sum_{k=1}^{K} d_k$. Desired signals are obtained by multiplying $\mathbf{y}_k$ with the postcoding vector, $\mathbf{D}_k$ with a size of $N_R \times q_k$. The decoded data symbols can be written as

$$\hat{\mathbf{y}}_k = \mathbf{D}_k^H\mathbf{y}_k \tag{4}$$

The spectral efficiency for stream i of user k is expressed as

$$\eta_{ki} = \log_2(1 + \gamma_{ki}), \tag{5}$$

where γ_{ki} is the SINR for the i^{th} stream of the k^{th} user and it is calculated as

$$\gamma_{ki} = \frac{(P_k/q_k)\alpha_{kk}^2\mathbf{d}_k^{iH}\mathbf{H}_{k\mathcal{M}_k}\mathbf{t}_k^i\mathbf{t}_k^{iH}\mathbf{H}_{k\mathcal{M}_k}^H\mathbf{d}_k^i}{\mathbf{d}_k^{iH}\mathbf{B}_{k\mathcal{M}_i}\mathbf{d}_k^i} \tag{6}$$
$$\forall k = 1, ..., K, \quad \forall i = 1, ..., q_k$$

where $\mathbf{t}_k^i$ is the i^{th} column vector of the precoding matrix $\mathbf{T}_k$ with dimension $N_T|\mathcal{M}_k| \times 1$, and $\mathbf{d}_k^i$ is the i^{th} column vector of postcoding matrix $\mathbf{D}_k$ with dimension $N_R \times 1$. Furthermore, $\mathbf{B}_{ki}$ is defined as the interference plus noise covariance matrix for the i^{th} stream of the k^{th} receiver and it is given by

$$\mathbf{B}_{ki} = \sum_{\substack{l=1,\\ l\neq i}}^{q_k} \frac{P_k}{q_k}\alpha_{kk}^2\mathbf{H}_{k\mathcal{M}_k}\mathbf{t}_k^l(\mathbf{t}_k^l)^H\mathbf{H}_{k\mathcal{M}_k}^H + \tag{7}$$
$$\sum_{\substack{j=1\\ j\neq k}}^{K}\sum_{q=1}^{q_j} \frac{P_j}{q_j}\alpha_{kj}^2\mathbf{H}_{k\mathcal{M}_j}\mathbf{t}_j^q(\mathbf{t}_j^q)^H\mathbf{H}_{k\mathcal{M}_j}^H + \sigma^2\mathbf{I}_{N_R},$$
$$\forall k = 1, ..., K, \quad \forall i = 1, ..., q_k.$$

Accordingly, the total *sum spectral efficiency* is as follows

$$\eta = \sum_{k=1}^{K}\sum_{i=1}^{q_k} \log_2(1 + \gamma_{ki}), \tag{8}$$

B. Problem Definition

The main objective is to minimize interference while identifying the optimal stream allocation scheme for each AP cluster and UE within the system. In this context, the stream allocation problem aims to maximize the total spectral efficiency of the network while ensuring that each user has at least one stream selected, thus guaranteeing service. Mathematically, this can be formulated as follows.

$$\left\{(\mathbf{T}_{\mathcal{M}_k}^*, \mathbf{D}_k^*)\right\}_{k=1,\ldots,K} = \underset{\mathbf{T}_{\mathcal{M}_k}, \mathbf{D}_k}{\text{argmax}}\ \eta \tag{9a}$$

$$s.t. \quad d_k \geq 1 \quad k = 1, ..., K \tag{9b}$$

where d_k is the number of assigned streams for user k.

To mitigate phase misalignment in CF-MIMO networks, existing methods cluster phase-coherent APs [4], [8]. However, inter-cluster interference persists due to the lack of alignment across clusters. Moreover, optimizing the number of streams per UE to balance throughput and interference remains an open problem. To bridge this gap, we propose a stream selection algorithm that achieves near-optimal performance comparable to exhaustive search methods but with significantly lower computational complexity.

III. The Proposed Framework

Motivated by the existing gap in the literature, this section presents a stream selection algorithm for a coherently clustered network aiming to optimize spectral efficiency and minimize interference in a CF-MIMO network. The proposed framework mainly consists of AP clustering and stream selection. First, APs are grouped into clusters based on proximity and reference distance, D_{ref}, as proposed in the studies of [4], [8]. Next, system parameters are initialized, and the corresponding cluster CSI is computed. The key contribution of this work lies in the stream selection phase, where inter-cluster interference is managed through orthogonal projections after each selection, suppressing interference both to and from the selected stream. The overall framework is summarized in Algorithm 1.

A. AP Clustering for Coherent Transmission

To enable mixed coherent and non-coherent transmission in distributed CF-MIMO networks, we cluster APs into non-overlapping, phase-aligned groups based on proximity and aggregate channel gain. This clustering mitigates phase misalignment caused by propagation delays and oscillator mismatches, allowing coherent transmission within clusters while maintaining non-coherent links across them. The clustering algorithm, adapted from [8] with enhancements for stream selection, constructs zones of neighboring APs within D_{ref}. At each step, the largest zone is selected, prioritizing those with the highest collective channel strength. Each UE is then associated with the cluster offering the strongest channel gain. The description of how inter-cluster interference is handled is in Section III-B. The procedure is detailed in Algorithm 2.

B. Interference Mitigation

In stream selection-based IA algorithms, each stream is chosen to lie in the null space of previously selected streams, ensuring interference avoidance.

Streams are computed using the Singular Value Decomposition (SVD) of all channels, $(\alpha_{kk}\mathbf{H}_{k\mathcal{M}_k}) = \mathbf{U}_k\mathbf{S}_k\mathbf{V}^H_{\mathcal{M}_k}$ where $\mathbf{U}_k$ and $\mathbf{V}_{\mathcal{M}_k}$ are orthogonal matrices representing receive and transmit beamforming directions at the UE and APs, respectively, and $\mathbf{S}_k$ contains the singular values indicating stream strengths. The l^{th} column vectors of $\mathbf{U}_k$ and $\mathbf{V}_{\mathcal{M}_k}$ are denoted by $\mathbf{u}^l_k$ and $\mathbf{v}^l_{\mathcal{M}_k}$.

To mitigate interference, IA techniques align the interfering components after each stream selection step. Two interference types are considered: (i) from the selected stream to remaining streams, and (ii) from remaining streams to the selected stream. Correspondingly, two virtual channels, Virtual Receiving Channel (VRC) and Virtual Transmitting Channel (VTC), are defined [9]. Precoding and postcoding matrices, constructed from the selected stream vectors, are expressed as: $\mathbf{T}_{\mathcal{M}^*_k} = [\mathbf{v}^1_{\mathcal{M}^*_k}, \ldots, \mathbf{v}^{q_k}_{\mathcal{M}^*_k}]$ and $\mathbf{D}_{k^*} = [\mathbf{u}^1_{k^*}, \ldots, \mathbf{u}^{q_k}_{k^*}]$. Then, interference is mitigated through orthogonal projections. For users $j \neq k$, the remaining beamformers are projected onto the null space of the selected stream's VRC and VTC, yielding projected matrices $\mathbf{H}^{\perp}_{j\mathcal{M}_j}$. At iteration i, interference from and to the selected stream is reduced by projecting channel matrices orthogonally to the respective virtual channels. The projection matrix is given by $\mathbf{P}^{\perp}_{\mathbf{x}} = \mathbf{I} - \frac{\mathbf{x}\mathbf{x}^H}{\|\mathbf{x}\|^2}$. The complete IA procedure is detailed in Algorithm 1 of [10].

Algorithm 1 The Proposed Framework Flow

Input: Set of APs, UEs, CSIs.
Output: AP clusters, selected streams, beamforming vectors.

Coherent AP Clustering by implementing **Alg. 2**.
Initialize system parameters and compute CSI.
Call **Alg. 3** to perform the proposed stream selection algorithm based on the formed clusters.

Algorithm 2 AP Clustering in PC Transmission

Input: AP positions, $\mathbf{h}_{kl}\ \forall k, l$, D_{ref}
Output: Set of clusters $\{\mathcal{M}_c\}$ and corresponding $\mathbf{H}_{k\mathcal{M}_c}\ \forall k, c$

For each AP l, define zone $\mathcal{Z}_l = \{l' \mid \|l - l'\| \leq D_{\text{ref}}\}$
while any zone $\mathcal{Z}_l$ has size > 1 **do**
  Find zones with maximum size $|\mathcal{M}_c|$
  Add selected zone to the clusters $\mathcal{M}_c$
  Remove its APs from all other zones
end while
for all $\mathcal{Z}_l \neq \emptyset$ **do**
  Define cluster $\mathcal{M}_c = \mathcal{Z}_l$
end for
for all formed clusters $\mathcal{M}_c$ **do**
  Construct $\mathbf{H}_{k\mathcal{M}_c}\ \forall k, c$
end for

C. Multi-Stream Transmission in CF-Networks

In this section, we propose a recursive stream selection procedure to determine the optimal beam combinations while incorporating the IA approach explained in sub-section III-B at each stream selection step. The process initializes multiple stream sequences, each beginning with the strongest stream for every cluster-user pair, defined as the one with the highest singular value of the channel matrix. The number of initialized sequences equals the number of cluster-user pairs, with the initial set, Ω_0, containing only the best streams of each pair.

After initializing the stream paths, the algorithm iteratively selects the stream from the available set Ω that maximizes spectral efficiency. If no stream improves efficiency at iteration i, the one causing the least decrease is chosen, prioritizing users with no assigned streams. The process continues until no more streams can be selected. The selected streams are kept in a set Ψ. At each iteration of the proposed *Comparative Stream Selection (CSS)* algorithm, the selected stream is transferred from Ω to Ψ, where all selected streams are accumulated. The whole process is given in Algorithm 3.

D. Complexity Analysis of Stream Selection-Based Algorithms

To benchmark the proposed algorithm, we derive an upper bound using exhaustive search, which evaluates all possible stream sequences. Its main drawback is the high computational complexity, which increases with the number of streams. Following the IA approach in [10], the complexity of stream selection algorithms can be compared based on the number of invocations of Algorithm 1. The worst-case complexity of this algorithm is $\mathcal{O}(K(NM^2 + N^2M + M^3))$ where $M = \max_{\forall k}(N_T)$ and $N = \max_{\forall k}(N_R)$ are the maximum transmit and receive antenna counts. The total number of invocations of the IA algorithm in the exhaustive search over all possible stream combinations is given as follows.

$$\sum_{i=K}^{r} \left(\underbrace{i! \left[\prod_{k=1}^{K} \binom{q_k}{1} \right] \binom{r-K}{i-K}}_{\text{Number of stream sequences}} \times \underbrace{i}_{\text{IA calls per sequence}} \right) \tag{10}$$

Algorithm 3 CSS Algorithm

Construct the initialization set Ω_0
  $\Omega_0 = \{(k,l)|\ k \in \Gamma \text{ and } l = 1\}$
Start constructing stream sequences
for each stream $(k^*, l^*) \in \Omega_0$ **do**
  Initialize the variables
    $\Psi = \emptyset$; $i = 1$; $d_k = 0$; finish = FALSE and
    $\mathbf{H}^{\perp}_{k_{k\mathcal{M}_k}} = \mathbf{H}_{k\mathcal{M}_k}$ for $k = 1, ..., K$
  Compute the SVD of all couples
    $\mathbf{H}_{k\mathcal{M}_k} = \mathbf{U}_k\mathbf{S}_k\mathbf{V}^H_{\mathcal{M}_k}$ for $k = 1, ..., K$
  Set the stream to be selected initially (k^*, l^*)
    $\Psi = \Psi \cup (k^*, l^*)$ and $d_{k^*} = d_{k^*} + 1$
  Perform IA by Algorithm 1 in [10].
  Construct $\Omega = \left\{(\mathbf{S}_k)(l,l)|k = 1, ..., K \text{ and } l = 1, ..., \mathbf{rank}(\mathbf{H}^{\perp}_{k\mathcal{M}_k})\right\}$
  Continue selecting streams by applying **Algorithm 2 in [10]**
  Compute $(\mathbf{T}_k)_\Psi$, $(\mathbf{D}_k)_\Psi$ and η_Ψ for stream sequence Ψ
end for
Select the best stream sequence according to Eq. (9a)
  $\Psi^* = \underset{\Psi}{\text{argmax}}\ \eta_\Psi$
  $\mathbf{T}^*_k = (\mathbf{T}_k)_{\Psi^*}$, $\mathbf{D}^*_k = (\mathbf{D}_k)_{\Psi^*}$ for $k = 1, ..., K$
Output: $\mathbf{T}^*_k$, $\mathbf{D}^*_k$ $\forall k$

TABLE I: System Parameters

Parameter Name	Parameter Value
Transmit Power of APs	30dBm
Bandwidth	50MHz
Noise Power	-174dBm/Hz
Noise Figure	7dB
Simulation Area	1×1km
Path loss [1]	$-30.5 - 36.7 \log_{10}\left(\frac{\text{dis}_{kl}}{1\text{ m}}\right)$dB
Shadowing std. dev.	4dB
Antenna number of each AP	4
Antenna number of each UE	2

By contrast, the CSS algorithm requires $K \times r$ invocations of the IA algorithm, resulting in significantly reduced complexity. The greedy selection method further reduces the number of invocations to at most $K \times N_R$.

IV. Performance Results

In this section, the performance of the proposed algorithm, CSS, is evaluated in a CF-MIMO system setup where users are independently and uniformly distributed in a 1×1km square area with a wrap-around topology. The minimum distance between each AP is 50m and $D_{ref} = 200$m. System parameters used in the simulations are listed in Table I.

Due to the high complexity of exhaustive search, we evaluated the upper bound only for a small-scale scenario ($L = 6$, $K = 4$), as shown in Fig. 1a. It can be observed that the Cumulative Distribution Function (CDF) at 0.9, CSS algorithm achieves a spectral efficiency of 36 bps/Hz, reaching 86% of the exhaustive search performance, demonstrating its near-optimal efficiency with significantly lower complexity. Additionally, CSS outperforms the greedy approach by 16%, highlighting the benefits of adaptive stream selection. It also surpasses fixed stream allocation schemes, emphasizing the importance of dynamically adjusting streams to network conditions. Notably, allocating all streams when $d = 2$ results in excessive interference, reinforcing the need for efficient stream selection. For the larger-scale scenario where $L = 24$ and $K = 6$, the CSS algorithm demonstrates once again a strong

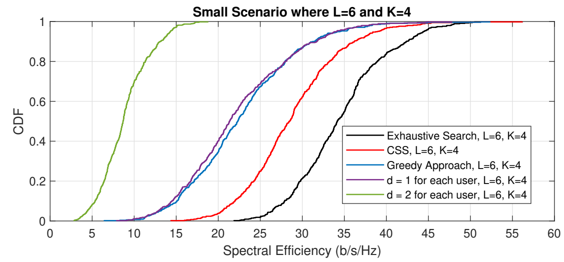

(a) Performance Comparisons in a small scenario ($L = 6$, $K = 4$)

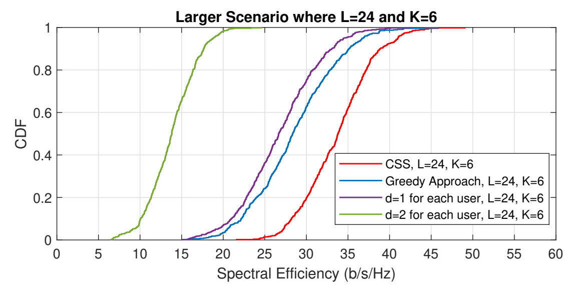

(b) Performance Comparisons in a larger scenario ($L = 24$, $K = 6$)

Fig. 1: Performance Comparison of CSS for different scenarios

TABLE II: Complexity Comparisons of different stream selection algorithms in terms of invoking Algorithm 1 in [10]

Algorithm	Small-scale scenario	Large-scale scenario
Greedy	2	2
CSS	4	6
Exhaustive	4.9×10^5	$\approx 9 \times 10^9$

performance, as illustrated in Fig. 1b. At CDF $= 0.9$, CSS achieves a spectral efficiency of 39 bps/Hz, outperforming the greedy approach by 11%. Similarly, the fixed resolution scheme remains far from optimal.

Additionally, Fig. 2 shows the CDF of the spectral efficiency for various stream selection approaches, analyzing the impact of interference mitigation and clustering strategies for $L = 12$ and $K = 4$. The results highlight significant differences in coherent and non-coherent clustering scenarios between the proposed CSS algorithm and the greedy stream selection approaches, both with and without IA. The complexity comparisons is given in Table II in terms of the number of calls to Algorithm 1 in [10]. At CDF $= 0.9$, the CSS algorithm with IA in coherent clusters achieves a spectral efficiency of 39 bps/Hz, outperforming the greedy algorithm with IA in coherent clusters by 18%. Similarly, the CSS algorithm with IA in non-coherent clusters achieves 35 bps/Hz, which is 17% higher than the greedy approach in non-coherent clusters. Furthermore, CSS with IA in coherent clusters provides a 11% improvement over CSS with IA in non-coherent clusters. Lastly, CSS with IA in coherent clusters outperforms both algorithms without IA by 44%, showing the impact of interference mitigation on improving spectral efficiency performance.

Fig. 3 presents the CDF of the sum spectral efficiency

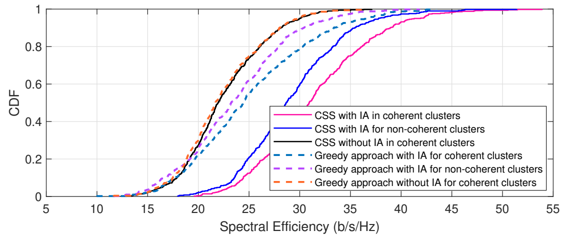

Fig. 2: Impact of coherent clustering and interference mitigation under different schemes on CSS and the greedy approach.

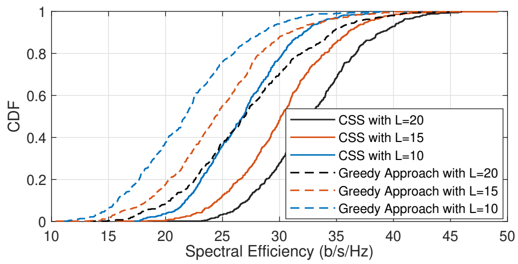

Fig. 3: Performance comparison of CSS and Greedy Approach for varying number of APs ($L = 10, 15, 20$) when $K = 5$.

for increasing number of APs ($L = 10, 15, 20$) with a fixed number of UEs ($K = 5$). As the number of APs increases, the CSS consistently outperforms the greedy approach, with the performance gap becoming more evident at higher percentiles. At the 90th percentile, CSS achieves 32 bps/Hz vs. 28.6 bps/Hz with greedy for $L = 10$; the gap increases to 4.85 bps/Hz at $L = 15$, and remains significant at 4.4 bps/Hz for $L = 20$. These results confirm the scalability and robustness of CSS in handling interference in denser AP deployments.

The average number of selected streams and the corresponding average spectral efficiency values in the small-scale CF-MIMO scenario, where $L = 6$ and $K = 4$, are compared for different numbers of receive antennas in Table III. The results show that increasing N_R enables more spatially multiplexed streams, directly improving the sum-rate and spectral efficiency.

V. Conclusion

In this letter, a novel stream selection framework is proposed for CF-MIMO networks with mixed coherent and non-coherent transmission. The method addresses phase misalignment and inter-cluster interference via dynamic stream allocation and interference mitigation. Simulation results confirm the effectiveness of the proposed CSS algorithm, achieving notable spectral efficiency gains across various network scales and interference conditions. Future work will address remaining challenges, for instance, establishing theoretical performance guarantees, such as approximation bounds. Moreover, recent advances in CPU-less and Reconfigurable Intelligent Surface (RIS)-assisted architectures [12] highlight the need for scalable, decentralized stream selection. Finally, in large-scale and dense deployments with mobile environments, learning-based clustering and AP-UE association enhance adaptability, especially when CSI is unavailable or imperfect, as is often the case in real-world scenarios.

TABLE III: Avg. number of streams and spectral efficiency for CSS and Greedy Search across different N_R values.

N_R	Algorithm	Avg. Streams	Spectral Efficiency (bps/Hz)
2	CSS	4.05	28.84
	Greedy	4.29	22.80
3	CSS	5.18	31.96
	Greedy	5.64	25.75
4	CSS	6.30	35.11
	Greedy	6.69	28.10

Acknowledgment

This research was supported by the 6G-TWIN project under the SNS JU Horizon Europe program with Grant Agreement No. 101136314.

References

[1] Özlem Tugfe Demir, E. Björnson, and L. Sanguinetti, "Foundations of user-centric cell-free massive mimo," *Foundations and Trends® in Signal Processing*, vol. 14, no. 3-4, pp. 162–472, 2021, doi: 10.1561/2000000109.

[2] E. G. Larsson, "Massive synchrony in distributed antenna systems," *IEEE Transactions on Signal Processing*, 2024, doi: 10.1109/TSP.2024.3358618.

[3] E. Shi, J. Zhang, J. An, G. Zhang, Z. Liu, C. Yuen, and B. Ai, "Joint AP-UE association and precoding for SIM-aided cell-free massive MIMO systems," *IEEE Transactions on Wireless Communications*, 2025, doi: 10.1109/TWC.2025.3546927.

[4] G. Li, S. Wu, C. You, W. Zhang, and G. Shang, "Asynchronous cell-free massive mimo-ofdm: Mixed coherent and non-coherent transmissions," *IEEE Communications Letters*, 2024, doi: 10.1109/LCOMM.2024.3518485.

[5] H. A. Ammar, R. Adve, S. Shahbazpanahi, G. Boudreau, and K. V. Srinivas, "Downlink resource allocation in multiuser cell-free mimo networks with user-centric clustering," *IEEE Transactions on Wireless Communications*, vol. 21, no. 3, pp. 1482–1497, 2021, doi: 10.1109/TWC.2021.3104456.

[6] J. Zheng, J. Zhang, J. Cheng, V. C. Leung, D. W. K. Ng, and B. Ai, "Asynchronous cell-free massive mimo with rate-splitting," *IEEE Journal on Selected Areas in Communications*, vol. 41, no. 5, 2023, doi: 10.1109/JSAC.2023.3240709.

[7] S. Kurma, K. Singh, P. Sharma, C. Li, and T. Tsiftsis, "On the performance analysis of full-duplex cell-free ma-mimo with user mobility and imperfect csi," *IEEE Transactions on Communications*, 2024, doi: 10.36227/techrxiv.21685361.v1.

[8] U. K. Ganesan, T. T. Vu, and E. G. Larsson, "Cell-free massive mimo with multi-antenna users and phase misalignments: A novel partially coherent transmission framework," *IEEE Open Journal of the Communications Society*, 2024, doi: 10.1109/OJCOMS.2024.3373170.

[9] M. Amara, M. Pischella, and D. Le Ruyet, "Enhanced stream selection for sum-rate maximization on the interference channel," *Wireless Communication Systems (ISWCS), 2012 International Symposium on*, pp. 151–155, 2012, doi: 10.1109/ISWCS.2012.6328348.

[10] E. Aycan Beyazıt, B. Özbek, and D. Le Ruyet, "On stream selection for interference alignment in heterogeneous networks," *EURASIP Journal on Wireless Communications and Networking*, vol. 2016, pp. 1–18, 2016, doi: 10.1186/s13638-016-0575-7.

[11] T. L. Marzetta, E. G. Larsson, H. Yang, and H. Q. Ngo, *Fundamentals of massive MIMO*. Cambridge University Press, 2016, doi: 10.1017/CBO9781316799895.

[12] W. Xu, J. An, H. Li, L. Gan, and C. Yuen, "Algorithm-unrolling-based distributed optimization for RIS-assisted cell-free networks," *IEEE Internet of Things Journal*, vol. 11, no. 1, pp. 944–957, 2023, doi: 10.1109/JIOT.2023.3288072.